Acta Oceanol. Sin., 2013, Vol. 32, No. 3, P. 10-18
DOI: 10.1007/s13131-013-0283-7
http://www.hyxb.org.cn
E-mail: hyxbe@263.net

Ocean current observation and spectrum analysis in central Chukchi Sea during the summer of 2008

CHEN Hongxia[1*], WANG Huiwu[1,2], SHU Qi[1,2], WANG Daolong[1,2], LIU Na[1,2]

[1] First Institute of Oceanography, State Oceanic Administration, Qingdao 266061, China
[2] Key Laboratory of Marine Science and Numerical Modeling, State Oceanic Administration, Qingdao 266061, China

Received 3 August 2012; accepted 30 October 2012

Abstract
During the summer of 2008, the third CHINARE Arctic Expedition was carried out on board of *Xuelong* Icebreaker in the central Chukchi Sea. A submersible mooring system was deployed and recovered at Station CN-01 (71°40.024′N, 167°58.910′W) with 33 days of the current profile records, and continuous observation of temperature and salinity data were collected. This mooring station locates in the blank of similar observation area and it is the first time for our Chinese to finish this kind of long-term mooring work in this area. This mooring system finished integrated hydrological observations with long-term continuous record of the whole profile velocity for the first time. Based on time series analysis of temperature, salinity, velocity and flow direction, we get the following main results. (1) During the observation period, the mean surface current velocity is 70.2 cm/s eastward, and velocity reaches its maximum in average at 3 m level with magnitude 90.0 cm/s, direction 206°. (2) In 9–30 m layers, the semidiurnal period variation is the most obvious, the flow direction is quite stable, and the flow is synchronous and consistent vertically. (3) Besides the semidiurnal period variation, the main variation in the upper layer is in 11-d period, with variations in period 5.5, 5.5, and 3.7 d, which reflect the influences of sea surface wind change and maintenance. (4) Near the bottom, the temperature change is correlated and synchronized with the conductivity.

Key words: Arctic Ocean, Chukchi Sea, submersible mooring system, long-term observations, spectrum analysis

Citation: Chen Hongxia, Wang Huiwu, Shu Qi, Wang Daolong, Liu Na. 2013. Ocean current observation and spectrum analysis in central Chukchi Sea during the summer of 2008. Acta Oceanologica Sinica, 32(3): 10–18, doi: 10.1007/s13131-013-0283-7

1 Introduction

As one of marginal seas of the Arctic, the Chukchi Sea locates in the northeast of the Chukchi Peninsula and northwest Alaska Peninsula, interlinks with the Pacific by the Bering in the South. It's northern border reaches to 76°N of the Arctic slope, connects with the East Siberia Sea through Delang Strait, and joins at Alaskay Barrow with the Beaufort Sea in the east.

Driven by the sea surface height difference between the Pacific and the Arctic (0.8–1.1 dyn m) (Coachman and Aagaard, 1966), Pacific water flows into the Chukchi Sea most of the time (Coachman and Tripp, 1970), and Chukchi Sea become the classics channel for the inflow Pacific water. Since there are two shoals such as Herald and Hanna in central area of the Chukchi Sea, the water flows mainly along the valley or channel (Paquette and Bourke, 1981), and under the influence of Taylor column effect generated by the seabed terrain, the inflow water from the Pacific divides into three branches in the Chukchi Sea (Fig. 1) (Weingartner et al., 1998).

Till 2008 China has completed 3 Arctic scientific expeditions and in each expedition the Chukchi shelf sea areas were investigated, research works of Chinese scholars in this area mainly focused on the Arctic water mass structure and sea ice characteristics. Gao, Dong and Shi (2003) analyzed the water mass of the Chukchi Sea in the summer of 1999 with the data collected in the first Chinese National Arctic expedition, he points out that shallow modified water mass dominates in this area, and the water mass includes two secondary water such as the summer Chukchi Sea water and the invasion water from the North Pacific. Tang's results (2005) indicate that, there are obvious regional differences between the Chukchi Sea water and Bering Sea water, and the temperature and salinity of Chukchi Sea water are lower than in those of Bering Sea water generally, a strong temperature and salinity front exists in the north of 70°N Chukchi Sea. In the Arctic sea ice research, Kang (2002) studied different combinations of the Chukchi Sea Ice structure with field observation data, and analyzed different thermodynamics processes in ice formation. With satellite remote sensing data, Zhu et al. (2005) and Hu (2007) studied the Chukchi Sea Ice variation and its dynamics mechanisms during the first and second Chinese Arctic scientific expedition respectively. Different time scale variations such as inter-annual and inter-decadal, and general trend of Chukchi Sea ice coverage during 1953–2004 were also studied.

Since the lack of field measured current data, the sea cur-

Foundation items: The National Key Basic Research and Development Plan under contract No. 2010CB950301: "Sea-ice-air interaction in the Southern Ocean and its influence on the south Indian Ocean", International Polar Year Chinese action plan project: "Chukchi Sea & Beaufort Sea ice anomaly variation and its impact on the winter climate of China"; National Science and Technology Support Program under contract No.2006BAB18B02: "Water masses and circulation monitoring technology and its application in the southern ocean"; The Basic Research Fund Project under contract No.FIO SOA 2010T01: "Key technology research of polar mooring observation system".
*Corresponding author, E-mail: chenhx@fio.org.cn.

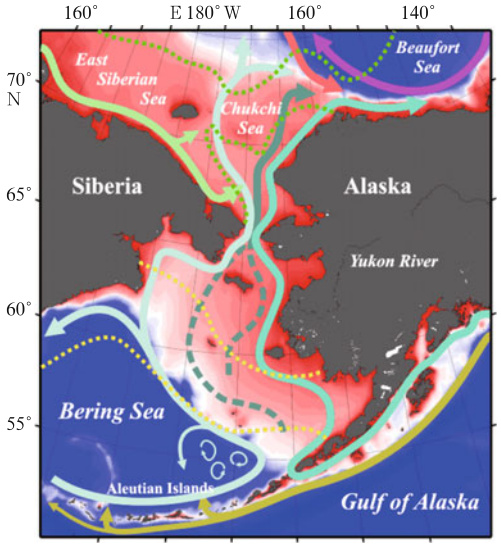

Fig.1. Flow diagram in the Bering Sea, Chukchi Sea and its adjacent waters (cited from Danielson et al., 2006).

rent study in the Bering Sea and the Arctic of Chinese scholars is mainly based on the dynamic analysis results (Gao, Dong, Zhao, et al., 2003). The earliest published Arctic hydrology research work based on measured current data was finished by Shi et al. (2004), a subsurface Arctic vortex was analyzed with continuous current profile data collected on an ice station of the second Arctic scientific expedition.

In view of the significance of the Arctic circulation and its branches in the study of Arctic (Zhao and Shi, 2004; Shi et al., 2004), as well as sea area where the Pacific water flow through is still weak in the research on the Chukchi Sea, the study of the circulation structure will benefit not only for the Pacific inflow route determination in the Arctic physically, but also for supporting in research of the influence of Pacific inflow on Arctic circulation, Arctic ocean dynamics balance and energy conversion studies.

2 Data

The submersible mooring observation system has great advantages such as long continuous recording, less susceptible to surface condition, and comprehensive observation elements, the mooring recordings are the highest value data in oceanographic research. With the technology development of long-term mooring system, Arctic coastal states in the Pacific sector (mainly the United States) began to set long-term observation systems in hydrodynamic environment investigation since 1990, totally 21 sites of long term observation data have been collected so far in the Chukchi shelf seas including the Bering Strait (Fig. 2). In terms of spatial distribution, the existed mooring sites are mainly concentrated in the Bering Strait and the Alaska northwest area east of 169°W. Among all of these sites, the earliest ones carried out ocean current observation in 1990 are A1 (65°54.00′N, 169°25.66′W), A2 (66°46.48′N, 168°35.23′W) and A3 (66°17.58′N, 168°57.89′W), which locate in the middle of Cape Dezhnev and the Diomede islands, in the middle of Diomede islands and Prince Welsh Cape, and the north of Diomede Islands respectively.

Since Russia joined in the long-term observation in 2003, the number of mooring systems in the Bering Strait increased to 7, and has been kept to date. These mooring systems constitute the observation array in study area which has the highest density and the longest duration, and provide a solid material foundation for research of substance and energy transport, hydrodynamic environment changes in the Drake Strait. The Bering Strait becomes the most prominent area in Arctic Oceanography research area (Weingartner et al., 2005; Woodgate et al., 2005; 2006).

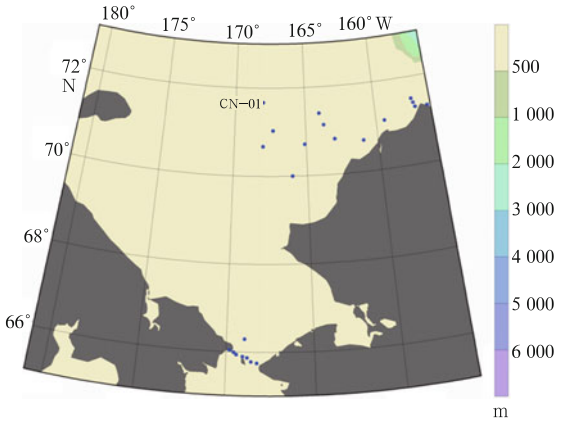

Fig.2. Mooring sites distribution in the Chukchi shelf sea and Bering Strait.

Compared with the work of America, Chinese Arctic research expedition and long term observation were carried out relatively later. Since 1999 when the first Chinese Arctic research expedition was carried out, 3 Arctic expeditions have been completed up to 2008. One mooring system has been deployed in the Bering Strait during the second Chinese Arctic research expedition (Jiao, 2008), and about 45 days of continuous velocity and temperature and salinity data was obtained at 2 layers for the first time. Constricted by relatively shallow water depth in the Bering Strait and the majority of the Chukchi Sea shelf, and effected potentially by sea surface ice and the vessel, current meters fixed on existed mooring systems are mostly for a single layer (AANDERAA current meter for instance), and mainly take current measurement in the middle and lower of the water column.

In the summer of 2008, the Acoustic Doppler Current Profiler (ADCP, 300 kHz) was mounted on the submersible mooring system for the first time during the third Chinese Arctic scientific expedition. The ADCP covered upper 32 m ocean current profile observation. Comparing with the former current meters, this ADCP recorded current profile within the upper ~10 m water column. The potential effects of the sea ice and the vessel were avoided, and direct current measurement was realized in the upper high velocity zone. This mooring system sited at CN-01 (71°40.03′N, 167°58.91′W), the north of Herald shoals, and in the northwest of the Chukchi Sea mooring system C1-91 (70°39.70′N, 167°00.90′W) deployed by the America in 1991. This station located in the blank area of existed anchor stations, and nearby the middle one of the three branches of the Pacific inflow in the Chukchi Sea.

The water depth is about 48.9 m at the mooring site CN-01, and the hydrologic station C11 (71°39.81′N, 167°58.87′W) is nearby. Before the mooring system was deployed, the CTD profiles at C11 were investigated and the results are shown in Fig.3. Main sensors and observation layers were set according

to the CT profile at C11. The mooring system is mainly composed of one ALEC Compact-CT HG, one RDI Workhorse Sentinel WHS300-I ADCP, two IXSEA acoustic releasers, 3 groups of floating buoys and 1 heavy metal anchor.

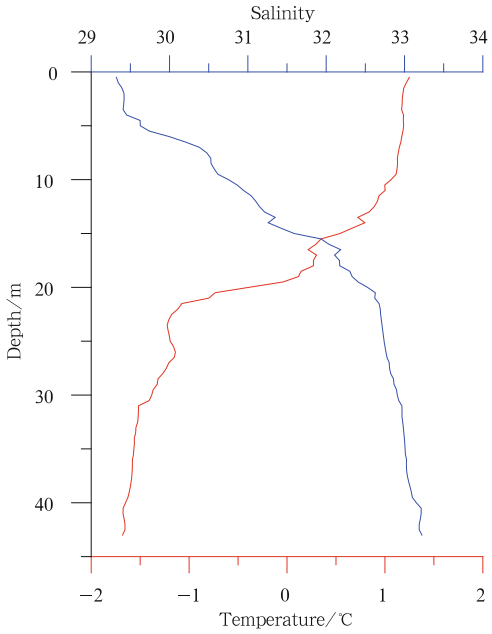

Fig.3. Temperature (red) and salinity (blue) profiles at Station C11 in the summer of 2008.

Two major types of data are used in this paper. One is the CT records of temperature, salinity data at 36 m depth which stands for the lower mixed layer. The effective work time of CT is from August 5th to September 7th, the total record time is 33.24 days with 1 minute sample interval. Removing records that collected on the deck, in the process of deploying and recovering, 4780 items of effective records are selected. As for the temperature record, its resolution is 0.001°C with the accuracy of ±0.05°C. For the conductivity data, its resolution is 0.001 mS/cm with the accuracy of ±0.05 mS/cm.

Another one is the profile data of velocity record collected by ADCP. As the actual depth of ADCP acoustic transducer depth of 37 m, and the first upward looking layer is 5 m above, with 3 m as the layer spacing distance in velocity profile, ADCP has recorded 12 layers of velocity data from 32 m (about 17 m to the bottom) upward to sea surface. Effective working time of ADCP is same to the CT with 1 minute time interval. The precision of velocity is 0.5 cm/s, the accuracy of flow direction is ±5°. The 12th layer is near the sea surface, acoustic echo signals might not be recovered at this layer, thereby part of the velocity records were missed because of tidal variation or surface fluctuations.

3 Character analysis and main results

Based on temperature, salinity records and velocity profile data, main hydrology characters and spectrum of this station are analyzed.

3.1 *Variation characteristics of temperature and conductivity*

Time series of temperature and conductivity at depth 36 m are shown in Fig. 4. If the inconsistent records with relatively low probability of occurrence are definite as singular value, it is clear that there are much more singular values in conductivity records, while less singular values in temperature records. Different working principles between temperature and conductivity sensors or the occurrence of short term (less than 10 min) dynamic process may be the main reason of this phenomenon. With the UNESCO freezing point formula, the freezing point is –1.47°C at depth of 36 m, while the measured temperature is about –1.5°C mostly. That means tiny ice crystals might appear around the sensor due to low environmental temperature, which can block the water exchange around the sensor. Since the conductivity sensor has worked in the low temperature environment for a long time, and the conductivity measurement needs relatively longer time to take record, abnormal conductivity data appeared as downward bulge. This raises new requirement for the technology of accurate conductivity measurement under weak hydrodynamic environment and freezing point circumstance.

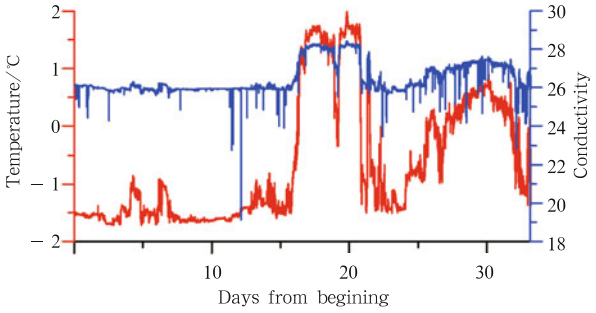

Fig.4. Temperature (red line) and conductivity (blue line) time series at the mooring station at depth 36 m (horizontal axis is the axis of time; the left axis is the axis of temperature; the right axis is the axis of conductivity).

The average value of temperature and conductivity are 0.64°C and 26.47 mS/cm during these 33 days of observation. While the maximum temperature is 1.98°C, and the minimum value is –1.71°C. The maximum conductivity is 28.42 mS/cm and the minimum value is 19.76 mS/cm. On the whole, both the temperature time series curve and the conductivity time series curve exhibit synchronous and correlated characteristics, while the average value of temperature is –1.5°C and that of conductivity is 26.1 mS/cm.

Regardless those singular data in conductivity records, the most significant fluctuation occurred in August 21th–26th in the time series curve, both temperature and conductivity appear great increase and decrease process simultaneously, and the rate of acceleration and deceleration are very high. During these 5 days, the amplitude of temperature fluctuation is over 3°C, and the amplitude of conductivity variation is 2.8 mS/cm. This fluctuation is not only an increase and decrease process simply, but includes several minor fluctuations with smaller amplitude and several transition processes.

The second notable change of the time series curves appeared just after August 29th, it is another increase and decrease process. Amplitude of temperature variation of this process is much smaller than last one, and rate of acceleration and deceleration are quite gently. The amplitude of temperature fluctuation is 2°C, and that of the conductivity is about 3 mS/cm. This process can be divided into two parts. Before September 4th, it is mainly manifested in adjustment and increase. While after

that, it is mainly a reduction process. The increase rate is slightly lower than the decrease rate.

The synchronous variation of temperature and conductivity has also occurred in August 4th, 6th and 18–19th. Significant increase and decrease of temperature and conductivity are also exhibited in these processes, both the amplitude and duration of variation are significantly less than those of the above two processes.

In addition to the synchronous and correlated variation of temperature and conductivity, there are also synchronous and negative correlated variation process in the time series curves with the increase of temperature and decrease of conductivity, and the process with only the decrease of conductivity while the temperature keeping to be even. Since the duration of these processes are quite short, they are not discussed here.

3.2 *Statistics of the current velocity*

In order to analyze the distribution of current velocity at all layers water, the statistics results of velocity record number at each layer in different scope are shown in Table 1.

Table 1. Statistics of record number in different magnitude scope at all layer

Magnitude scope/cm·s^{-1}	1	2	3	4	5	6	7	8	9	10	11	12
[0–5)	16 578	6 423	6 255	6 488	6 680	7 277	5 961	5 219	4 977	717	234	729
[5–10)	21 325	14 996	15 029	15 733	17 183	16 347	15 010	14 278	13 462	2 158	802	1 961
[10–15)	8 008	12 997	14 126	15 862	14 909	14 504	15 958	14 510	14 010	2 716	1 016	2 490
[15–25)	1 832	12 736	11 653	9 109	8 351	8 893	9 771	12 190	13 194	7 584	1 284	4 065
[25–50)	59	650	739	610	679	781	1 102	1 605	2 154	26 643	2 353	8 082
[50–100)	0	0	0	0	0	0	0	0	5	7 909	21 067	18 913
[100–150)	0	0	0	0	0	0	0	0	0	69	20 840	8 565
[150–250)	0	0	0	0	0	0	0	0	0	6	206	2 664
[250–634)	0	0	0	0	0	0	0	0	0	0	0	333

As shown in Table 1, the velocity range of the surface layer (12th layer) is the widest, and the maximum velocity is 634 cm/s. The number of velocity record in scope of [250–634 cm/s) takes only 0.7% in all records, while that in [150–250 cm/s) takes 5.6%.

Considering the depth and parameters settings of ADCP, combining with the statistics number distribution of velocity (Fig. 5), it's true that sometimes the surface velocity is over 150 cm/s, and these records also are influenced greatly by the sea surface meteorological condition and fluctuations. There are two peak areas in the right picture of Fig. 5, while the number of velocity within [50–100 cm/s) is the largest of all subsections in table 1. It is very clear that 60–80 cm/s dominate in sea surface velocity magnitude, with ∼15 cm/s as auxiliary. The high frequency fluctuation of the distribution curve also reflects the influence of meteorological conditions and erratic sea surface factors. The averaged surface velocity is 70.2 cm/s and averaged current direction is 192°.

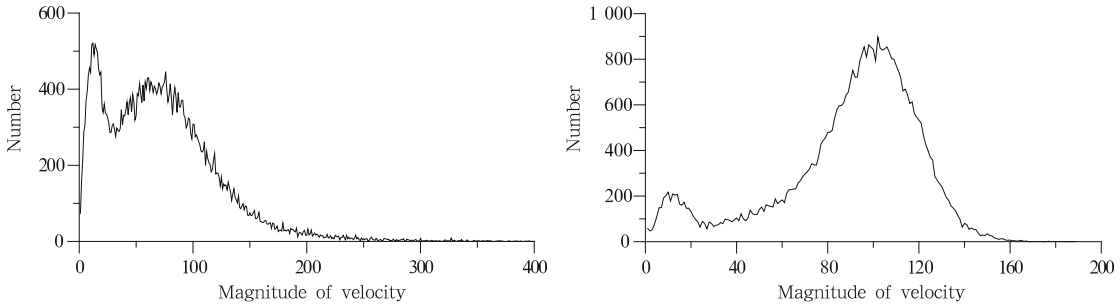

Fig.5. Record number statistics distribution of velocity magnitude at the twelfth (left) and eleventh (right) layer.

The velocity range at the eleventh layer is much narrower than that at the twelfth layer and the maximum velocity is 190 cm/s. The number of velocity records that greater than 150 cm/s is 206, which is only 6.8% of that at the surface layer. It reflects the rapid decay of velocity magnitude under the sea surface, and the limited effects from the sea surface factors and processes on this layer. The number of velocity record that in range of [50-100 cm/s) and [100–150 cm/s) are 21067 and 20840 respectively, and the sum account for 87.7% of the total. This exhibits a high velocity characteristic at the depth of 3 m. Further combination with the left picture of Fig. 5, the maximum number value of velocity record appears at about 100 cm/s. The average velocity of this layer is up to 90 cm/s, and the average flow direction is 206°. The high average velocity shows that this mooring station may be around the flow branch in the Chukchi Sea.

In the depth range of 12–32 m, the maximum velocities are less than 50 cm/s at all layers. With the increase of the depth, the number of velocity record that in range of [25–50 cm/s) decreases gradually.

Except the 32 m layer, velocity records at each other layer are concentrated in the range [5–25 cm/s) with the average velocity about 11.5 cm/s. In each subsection, the number of velocity at each other layer is similar. While at the 32 m layer, the number of velocity record reaches its maximum in range [0–5 cm/s), and the average flow is 8.1 cm/s. This shows the low cur-

rent characteristics of near sea bottom affected by the bottom friction, although the distance between 32 m layer and the sea bottom is about 17 m. The velocity is quite consistent and stable in the depth range of 15–29 m, which is out the range of sea surface meteorological influencing. With the increase of the depth, the velocity presents the feature of slow decrease downward.

At the layer at about 9 m, the averaged velocity is about 35.1 cm/s. There are velocity records greater than 50 cm/s, though the number is only 5. At the same time, velocity records fall in [25–50 cm/s) are much more than those at the eighth layer.

While at the layer of 6 m, the maximal velocity subsection is [150–250 cm/s), and number of records is only 6. Significantly different from that at the ninth layer, the number of velocity records reaches its peak in range of [25–50 cm/s), and the velocity is much higher. Combined with Fig. 6, the statistical distribution curve of velocity at 9 m is similar to that at 15 m, which reflects the approximate velocity feature to those at the 2–8 layers. The tenth layer is the transition layer from the top down, it is between the ninth and eleventh layer both in the peak velocity distribution and the roughness of the distribution curve.

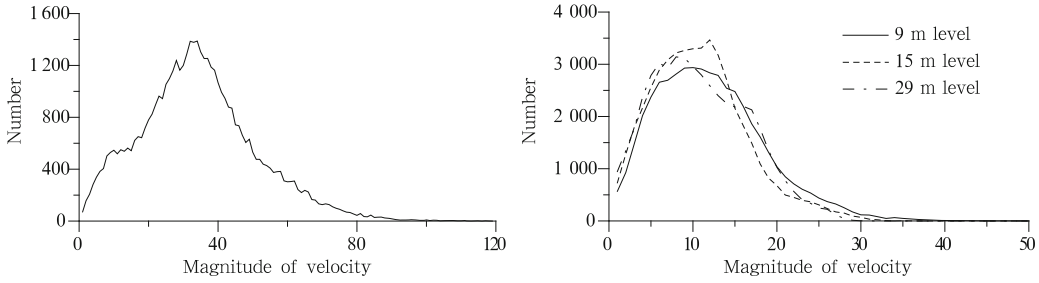

Fig.6. Number distribution of velocity magnitude at the depth 6 m (left), at depth 9 m, 15 m and 29 m (right).

3.3 *Velocity profile feature analysis*

To display the variation of velocity and current direction more clearly, ignoring velocity records that speed is over 150 cm/s, time sequence contours of velocity and current direction profiles are given from August 5, 2008 to September 7 in Fig. 8, and the time window of each contour is 5 days.

On the whole, the velocity is small and the flow direction is stable (mainly north, northeast and east) lower than 9 m. The flow direction is similar vertically and its variation is synchronous significantly with semidiurnal period. Based on the variation of sea surface wind (Wang et al., 2011), and according to the main characters of velocity profile and its variation, the observation can be further divided into three periods.

A) Aug. 5th–10th, 12th–22th, Aug. 30th–Sep. 6th. The main current direction in these 3 sub periods is southwest, and the current has the following characteristics.

As shown in Fig. 7, the most significant characteristic in these sub periods is that the profiles of both velocity and flow direction are consentaneous vertically below 9 m. The difference of averaged velocity at all layers is very small in the depth range of 9–29 m, and the velocity varied synchronously.

From the point of variation period, although there are dramatic color changes in the contour of flow direction when the flow direction is mainly northward, the variation of velocity and flow direction are very consistent with semidiurnal period. Affected by the bottom topography, the velocity decreases near the bottom, while its synchronization with upper layers is still very clear.

If the vertical differences of velocity and flow direction are focused on, there is a characteristic top-down counterclockwise rotation. This feature is the most significant during Aug. 12th–22th, when the wind is most stable.

During these sub periods, the velocity is high in upper 6 m averagely, and the current direction is mainly west and southwest. The maximum velocity 634.3 cm/s emerges at the top layer in Aug. 14th, and the corresponding current direction is 271°. The averaged velocity maximum 90 cm/s appears at depth 3 m, which is slightly larger than that of the surface (70.6 cm/s), and twice as that at depth 6 m (34.9 cm/s).

The distribution of current direction is more concentrated at 3 m and 6 m comparing with that at the surface layer. The current direction is most stable at 3 m, it ranges from 233° to 262°, which reflects the southwest-west strong flow characteristic under the force of the southwest wind. At depth of 6 m, the current direction ranges from 214° to 332°, which is relatively wide than upper layers. Hereafter the current has begun to have northward flow characteristics in lower layers, and the semidiurnal period variation begins to appear.

B) From Aug. 10th to 12th.

As shown in Fig. 7, continuous low value of velocity profile has appeared during this period. Although the maximum velocity reaches 84.4 cm/s at depth 3 m, the average velocity is only 28.8 cm/s, only one fourth of that in last period. Although the maximum velocity in range of depth 9–29 m is similar to that of last period, the velocity at 32 m keeps less than 5 cm/s, but there are almost no flow record less than 5 cm/s, and the semidiurnal variation is not obvious any more. At the same time regularity of the current direction weakens, the main direction change to be south and southeast. The flow direction below 12 m is relatively stable, it maintains north and northeast.

At August 9th the wind direction changed from southwest to south, and south is the main wind direction, which is opposite to the main current direction below 9 m. From 10th, the flow above 6 m decreased after 2 times of wind direction change, and recovered in the mid-late of this period. The periodic feature weakened both in velocity and direction below 9 m after that, which embodies the effect of sea surface wind to the whole velocity profile.

C) From Aug. 22th to 30th. The main wind direction is north in this period, and has experienced a series of wind changes, and the time consistency of wind direction is relatively poor.

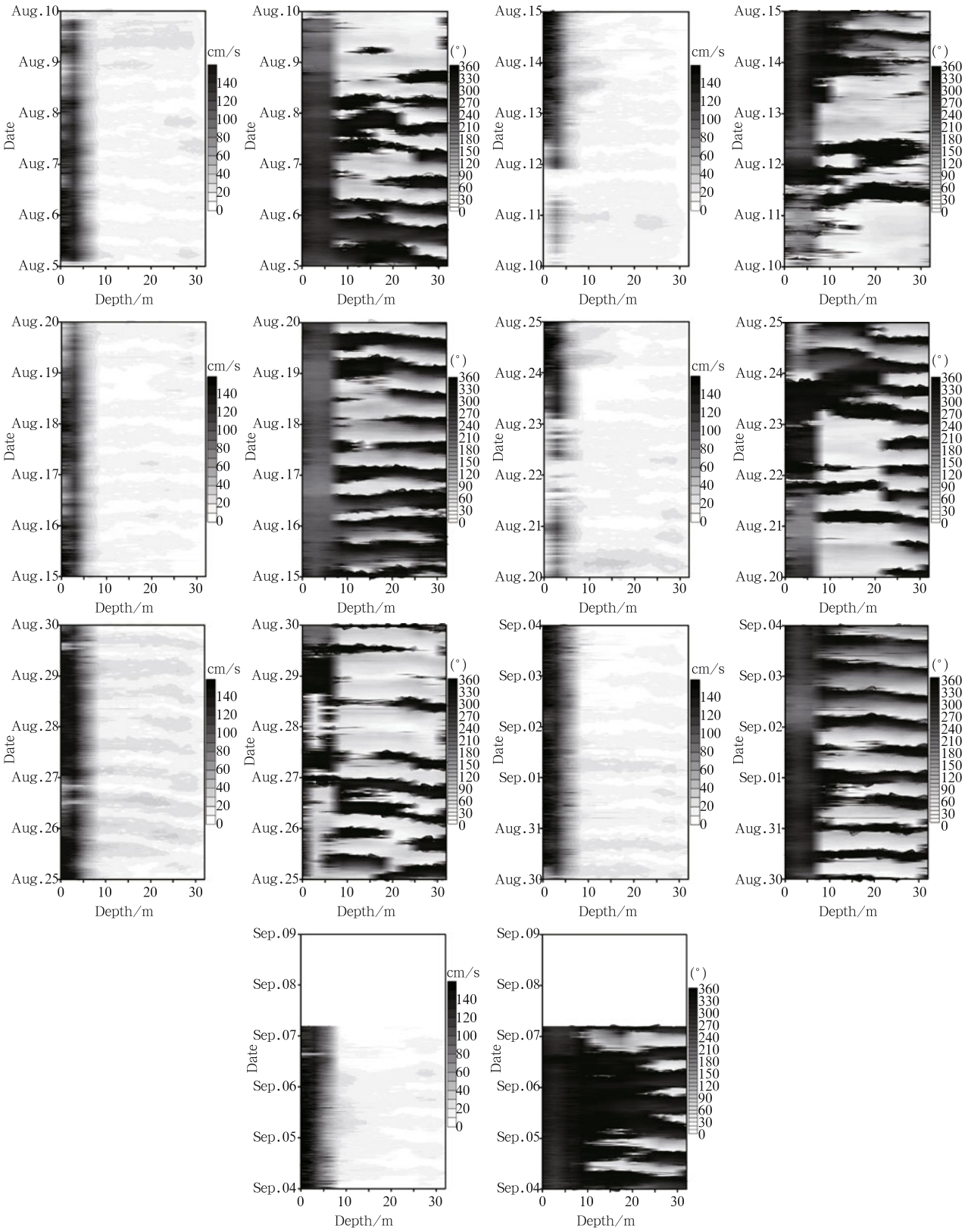

Fig.7. Distribution of velocity and current direction during Aug. 5th–15th, 2008; Distribution of velocity and current direction during Aug. 15th–25th, 2008; Distribution of velocity and current direction during Aug. 25th–Sep. 4th, 2008; Distribution of velocity and current direction during Sep. 4th–7th, 2008.

The velocity is less than the average at each layer above 6 m around Aug. 22th when the wind direction changes and the wind speed is low. The average velocity at the surface layer is 17.7 cm/s, 42.6 cm/s at depth 3 m, and 23.1 cm/s at depth 6 m, which are much smaller than those in other time periods. Along with the wind direction changes on August 27th, the flow in upper layers responses accordingly, and there are two significant weakening processes in the velocity profile.

Both the velocity and current direction are similar below 9 m, and have the synchronous variation character vertically. The periods of velocity and flow direction are semidiurnal, which is similar to that when the main wind direction is southwest.

The averaged velocity at each layer is approximate to that of the first period and that of the whole observation period. The main current direction is south-southeast now above 6 m, the direction angle with the surface wind is quite large, and different from that of other periods. The averaged current direction below 9 m layer changes from the northeast to the east correspondingly.

3.4 *Results of the spectrum analysis*

For further study of the current time-varying characteristics at the mooring station, and ignoring the changes less than 1 hour period, the Fast Fourier Transform is used in time series velocity records of each layer which are smoothed at 61 points.

A) The upper layers. According to the left picture of Fig. 9, the power spectrum distribution characteristics are basically consistent from sea surface to 6 m, and layers above 6 m is regarded as upper layers.

The peak of the power spectrum in each upper layer appears at 264 h (11 d), and this value exceeds the secondary maximum more than 3 times, which indicates that the major variation period is 11 days and embodies the dominant influence of the most stable wind during Aug. 11th–22th.

The sea surface secondary maxima of the power spectrum emerges at 132 h (5.5 d), which embodies several processes of wind direction, wind speed change with period of 5–6 days at sea surface. Although the secondary maximum appears at 132 h also of the 3 m layer, it is no more than 1/7 of the maximum. This presents the synchronization between 3 m layer and surface, and the energy concentration at depth 3 m.

Different from the upper two layers, the secondary maximum value at depth 6 m emerges at 88 h (3.7 d), where the third maximum value positions above. This value is about 1/5 of the maximum value, and it reflects the effect of 3–4 days weather process on the current.

B) Layers between 9–33 m. For convenience of presentation, the power spectra of layers between 9–15 m are given in the right of Fig. 8, while those of layers between 18–24 m, 27–33 m are given in the left and right pictures of Fig. 8 respectively. Taking variations within period of 200 h into consider, these 9 spectrum curve are similar both in trend and in the magnitude, this validates the flow profile synchronization further.

Different from the upper layers, the maximum value at all of these layers emerges at around 12.45 h. The period matches with the M_2 tidal period (12.42 h), and close to the local inertial period (12.6 h). At the period of K_2 and S_2 tide (11.96 h, 12 h), the spectrum value is only about 1/7–1/5 of the peak. It suggests that the local M_2 tide dominated the semidiurnal period variation, and the K_2 and S_2 tidal variation are included partially. As the local inertial period is consistent with the M_2 tidal period, under the action of inertia, semidiurnal periodic characteristic was further strengthened.

The distribution of the second maximum value is different at each layer. It appears near 132 h at layers between 9-15 m, decreases gradually up to down. At layers below 18 m, the third largest value locates at about 132 h, while the second maximum value is located near 78 h. It not only embodies the downward transfer of upper ~5.5 d periodic feature, but also exhibits the existence of the ~3 d period variation.

At 3 layers about 33 m and its adjacent above, not only the peak value of power spectrum around 12.45 h is much larger than those of the upper 6 layers, and the value near 78 h is relatively large. The absolute dominance of the semidiurnal variation and obvious period circle of ~3 d are very clear.

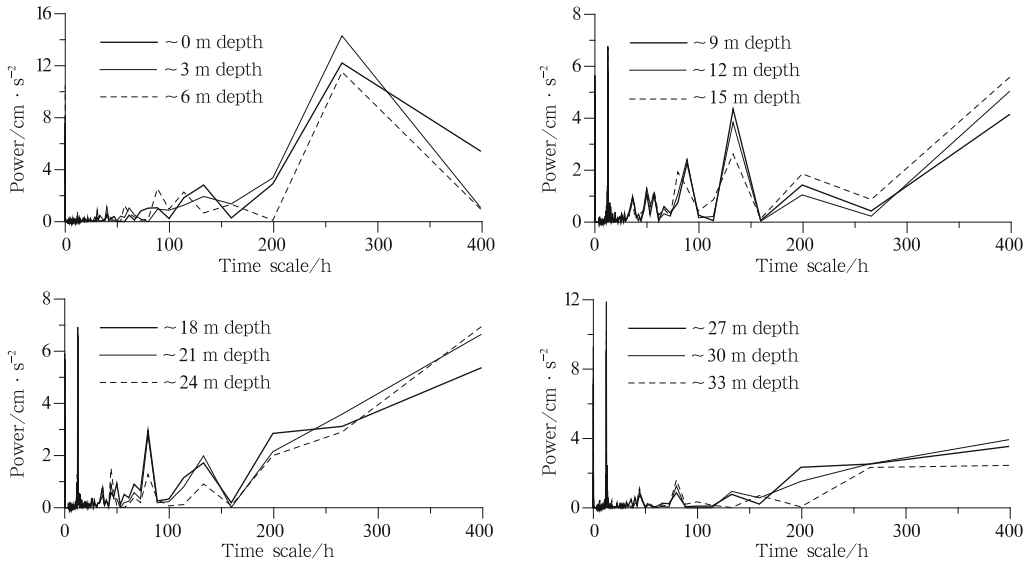

Fig.8. Spectrum curves of velocity at different layers between 0–6 m (left) and 9–15 m (right); spectrum curves of velocity at different layers between 18–24 m (left) and 27–33 m (right).

4 Conclustions

According to the above analysis results, the main conclusions can be reached at the mooring station in the summer of 2008 as follows:

(1) Temperature and conductivity time series are positive correlated and synchronous obviously at depth 36 m. The appearance possibility of ultra low temperature water is 32.4%. The average value of temperature and conductivity are 0.64°C and 26.47 mS/cm, while the maximum and minimum of temperature are 1.98°C and –1.71°C, the maximum and minimum of conductivity are 28.42 mS/cm and 19.76 mS/cm.

(2) Influenced greatly by meteorological condition and fluctuations of sea surface, surface velocity maximum is up to 634 cm/s, the average velocity is of 70.2 cm/s while the average direction is 192°. The average velocity reaches its maximum at depth 3 m, it is over 90 cm/s with direction of 206°. The 6 m layer is the transition layer from the top down, both the roughness of distribution curve and averaged velocity are between those of 3 and 9 m layer.

(3) The main period in layers above 6 m is 11 days, which embodies the dominant influence of the stable wind in Aug. 11th–22th. At these three layers, the second period of velocity variation are 5.5, 5.5, 3.7 days respectively from the top down, which reflects the influence of weather changes in scale of 3–6 days on the flow.

(4) The average velocity difference among layers between 9–30 m is quite small, and the current direction is relatively stable (mainly north, northeast and east) and similar, the semidiurnal period variation is obvious and synchronous. The velocity at 33 m is quite small with average value 8.1 cm/s, which shows the feature of near bottom current that subjected to the bottom friction.

(5) All peaks of power spectrum at layers between 9–33 m appear at around 12.45 h, which coincide with the period of the M_2 tide and close to the local inertial period. This indicates that the local M_2 tidal current is the dominated variation, together with the inertia effect, the semidiurnal periodic characteristic is strengthened further.

5 Discussions

Due to the statistical results are related with instrument settings, data sampling interval, statistical methods, data processing and data selection method, especially it is very artificial in the identification and elimination of abnormal values, results in this paper are based on the all the sampling data without any abnormal value filtering. There have certain differences with previous research in specific values.

For example, the velocity at layer 15 m is between 0–37.9 cm/s, and the average velocity is 12.0 cm/s in direction of north, northeast and east. Comparing with shipboard ADCP observation results in the north of Herald Shoal at 14 m (10–20 cm/s, (Weingartner, 2005)), the range of velocity is slightly larger and the main current direction also have certain difference. This is due to different measurement method, different observation positions, and the local sea surface meteorological condition has changed.

In addition, comparing with the current records collected near the bottom layer at the mooring station C1 west of the Herald Shoal (Weingartner, 2005), the average velocity magnitude is very close with relatively large current direction differences. It suggests that the near flow near the bottom is influenced by the seabed terrain, and that the 2 observation stations are at different flow paths.

In corresponding time, the main current direction at layers above 6 m is not consistent with the sea surface wind direction, which embodies the jointed action on the upper current from sea surface wind stress, the Pacific-Arctic pressure gradient force, as well as other current such as the southward flow in the central route.

Limited by the time length of observation and the empty of temperature-salinity observation in upper layers, hydrological characters analysis at the surface and thermocline, and variations over period over 15 days are absent in this paper. As the lowest observation layer is still 17 m to the bottom, the bottom current analysis need to be further corroborated by more information. This submersible mooring system accumulates experience for future development of mooring observations in the future, but also proposes new requirements for the construction of observation platform, observation elements and layers in nest step.

In addition, because of the lack of direct sea surface meteorological observation, there is a certain distance between the mooring station and the nearest grid where the satellite sea surface wind data is used. On the other hand, the time interval of satellite record is much higher than that of the mooring records. These factors affected on the relationship analysis between the sea surface wind and the current to some extent.

Furthermore, the mooring point has certain distance from the historical mooring point, the CN-01 station locates in the north of the Herald Shoal while Herald Shoal C1 is in the west. In Woodgate et al. (2005) only current results at layers 40 m and 45 m of C1 were given, the current in upper layers is in lack. Although Woodgate et al. (2005) have given the current near 14 m with shipboard ADCP records, still missing current records in upper 6 m.

References

Coachman L K, Aagaard K. 1966. On the water exchange through Bering Strait. Limnology and Oceanography, 11: 44–59

Coachman L K, Tripp R B. 1970. Currents North of Bering Strait in Winter. Limnology and Oceanography, 15: 625–632

Danielson S, Aagaard K, Weingartner T, et al. 2006. The St Lawrence polynya and the Bering shelf circulation: New observations that test the models. Journal of Geophysical Research, J111: C09023, doi:10.1029/2005JC003268

Gao Guoping, Dong Zhaoqian, Shi Maochong. 2003. Water properties of the seas surveyed by Chinese first Arctic research expedition in summer, 1999. Chinese Journal of Polar Research, 15(1): 11–20

Gao Guoping, Dong Zhaoqian, Zhao Jinping, et al. 2003. Dynamic analysis of current over the continental slope of the east Bering Sea in summer, 1999. Chinese Journal of Polar Research, 15(2): 91–101

Hu Xianmin, Su Jie, Zhao Jinping, et al. 2007. Variation characteristics of the sea ice extent in Bering-Chukchi Seas. Journal of Glaciology and Geocryology, 29(1): 53–60

Jiao Yutian, Zhao Jinping, Shi Jiuxin, et al. 2008. Design and deployment of anchorage surveying flow system in Polar Region. Ocean Technology, 27(1): 22–25

Kang Jiancheng, Sun Bo, Sun Junying, et al. 2002. The characteristics of summer sea ice and their relationship with climate in the Chukchi Sea. Journal of Glaciology and Geocryology, 24(2): 173–180

Paquette R G, Bourke R H. 1981. Ocean Circulation and Fronts as Related to Ice Melt-back in the Chukchi Sea. Journal of Geophysical Research, 86(C5): 4215–4230

Shi Jiuxin, Zhao Jinping, Jiao Yutian, et al. 2004. Pacific inflow and its links with abnormal variations in the Arctic Ocean. Chinese Journal of Polar Research, 16(3): 253–260

Shi Jiuxin, Zhao Jinping, Jiao Yutian, et al. 2008. Structure of a subsurface eddy in Canadian Basin of Arctic Ocean. Chinese Journal of Polar Research, 20(1): 1–13

Tang Yuxiang, Jiao Yutian, Zou Emei. 2005. A preliminary analysis of the hydrographic features and water masses in the Bering Sea and the Chukchi Sea. Chinese Journal of Polar Research, 17(1): 11–22

Wang Huiwu, Chen Hongxia, Lü Liangang, et al. 2011. Study of the tide and residual current observations in Chukchi Sea in the summer 2008. Acta Oceanologica Sinica(in Chinese), 33(6): 1–8

Weingartner T, Aagaard K, Woodgate R, et al. 2005. Circulation on the North Central Chukchi Sea Shelf. Deep-Sea Research, 52(24–26): 3150–3174

Weingartner T J, Cavalieri D J, Aagaard K, et al. 1998. Circulation, dense water formation and outflow on the northeast Chukchi Sea shelf. Journal of Geophysical Research, 103: 7647–7662

Woodgate R A, Aagaard K, Weingartner T J. 2005. Monthly temperature, salinity, and transport variability of the Bering Strait throughflow. Geophysical Research Letters, 32(4): L04601, doi:10.1029/2004GL021880

Woodgate R A, Aagaard K, Weingartner T J. 2006. Interannual changes in the Bering Strait fluxes of volume, heat and freshwater between 1991 and 2004. Geophysical Research Letters, 33: L15609, doi:10.1029/2006GL026931

Zhao Jinping, Shi Jiuxin. 2004. Research progresses and main scientific issues in studies for Arctic circumpolar boundary current. Chinese Journal of Polar Research, 16(3): 159–170

Zhu Dayong, Zhao Jinping, Shi Jiuxin. 2005. Differences of sea ice distribution in Chukchi Sea and the dynamic mechanism in 1999 and 2003. Chinese Journal of Polar Research, 17(1): 11–22